DIELECTRICALLY-LOADED WAVEGUIDE AS A MICROWAVE UNDULATOR FOR HIGH BRILLANCE X-RAYS AT 45 – 90 keV*

R. L. Kustom, G. Waldschmidt, and A. Nassiri
Argonne National Laboratory, Argonne, IL, USA

Abstract

The HEM_{12} mode in a cylindrical, dielectrically-loaded waveguide provides E and H fields on the central axis that are significantly higher than the fields on the conducting walls. This structure, operating near the cutoff frequency of the HEM_{12} mode, spans a frequency range where the wavelength and phase velocity vary significantly. This property can be exploited to generate undulator action with short periods for the generation of high brightness x-rays. The frequency range of interest would be from 18 to 34.5-GHz. The goal would be to generate x-rays on the fundamental mode over a range of 45 to 90-keV.The tunability would be achieved by changing the source frequency while maintaining a constant on-axis equivalent undulator field strength of 0.5-T.

INTRODUCTION

The ability to generate x-rays with high brilliance on the fundamental mode in the range of 45 to 90-keV with permanent magnet and superconducting wire undulators is a balancing act between vacuum aperture and adequate undulator field. In most cases, the higher energies are generated on higher harmonics of the undulator. A microwave undulator (MU) can provide the advantage of larger vacuum apertures, up to 3 to 5 cm, with subcentimeter undulator periods and strong on-axis fields.

Microwave undulators were first proposed by Shitake at KEK [1] and Batchelor at BNL [2]. Recently, corrugated WGs have been investigated as undulator structures [3]. A room temperature MU that operates in pulsed mode with tens of MW of input power has been demonstrated at SLAC [3]. The device generates a 0.65-T equivalent undulator field.

A dielectrically-loaded waveguide (WG) generates transverse fields that would be suitable for undulator action [4,5]. The WG structure is a cylindrically symmetric tube shown in Fig. 1. The inner radius of the dielectric is a, the conducting wall is at the outer radius, b, and dielectric is between radii a and b.

The HEM_{12} mode in the dielectrically loaded WG is the sum of a TE and TM mode for which the velocity of propagation is identical for each of those modes and for which the fields are matched at the dielectric boundary.

*Work supported by the U. S. Department of Energy. Office of Science under Contract No. DE-AC02-06CHI 1357

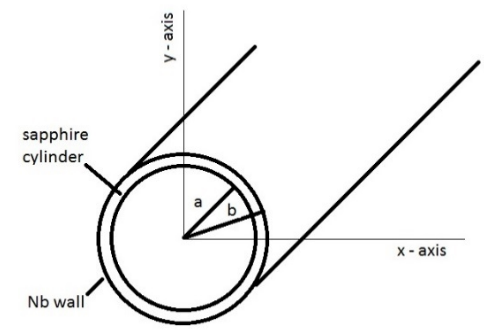

Figure 1: Geometry of a cylindrical dielectrically loaded WG.

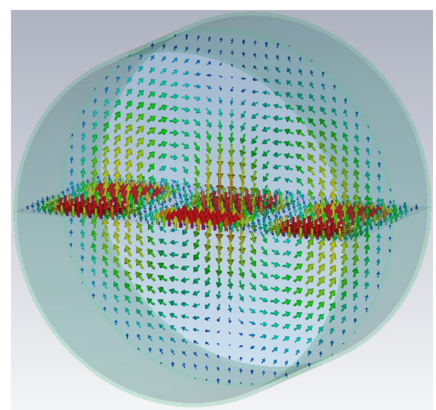

Figure 2: Electric field plot for HEM_{12} mode.

Figure 2 is a Microwave Studio generated plot of the transverse H-field for the HEM_{12} mode at 18-GHz while Fig. 3 shows the field components in the HEM_{12} mode. The E fields at the conducting walls, at a radius of 22 mm, are very low relative to the E fields on the axis.

UNDULATOR ACTION

The E and H fields of the HEM_{12} mode are strong on the axis compared to values on the walls as well as on the dielectric vacuum interface. This makes the mode very efficient because high deflecting fields are generated with comparatively low losses. Other field values for this mode are zero on the axis [4,5].

A charged particle traveling on the WG axis in the direction towards the oncoming wave experiences the transverse deflecting force, F_d, shown in Eq. (1).

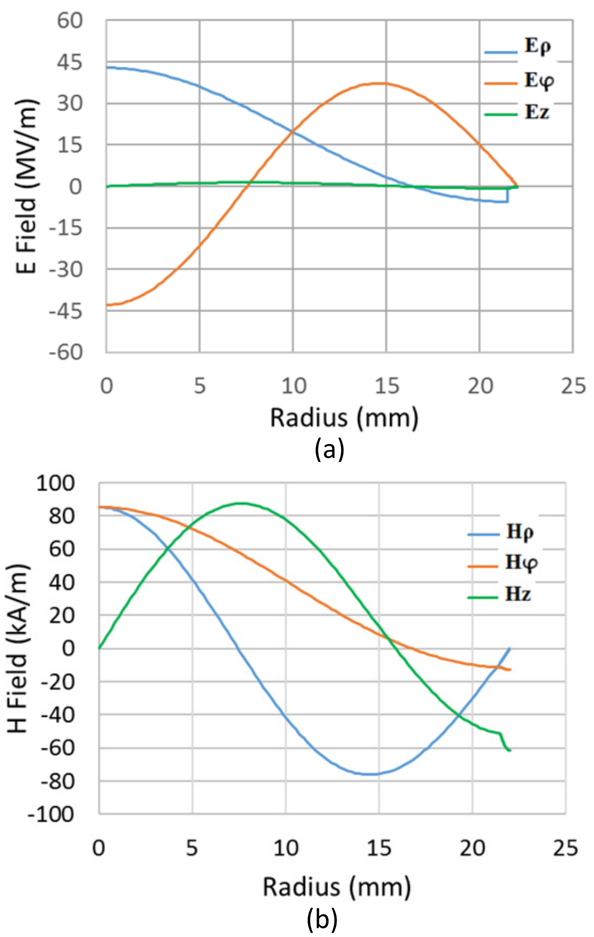

Figure 3: Field components for a HEM_{12} mode along radial direction: (a) Electric Field and (b) Magnetic intensity.

$$F_d = q\,(E_x + v\,\mu_0\,H_y), \tag{1}$$

where q is the charge of the particle, E_x and H_y are the on-axis fields, v is the particle velocity and μ_0 is the permeability of free space.

The equivalent undulator field, B_u, for a static magnet array to create the same deflection as the MU is given in Eq. (2):

$$B_u = E_x/v + \mu_0\,H_y \tag{2}$$

A WG has a cutoff frequency for any given mode below which the wave will not propagate. The cutoff frequency, f_c, is determined by its transverse geometry. The phase velocity of the EM wave, v_p, at the operating frequency, f, is related to f_c and the speed of light, c, as shown in Eq. (3):

$$v_p = c\,/[1 - (f_c/f)^2]^{1/2} \tag{3}$$

The guide wavelength, λ_g, is the distance for which the phase advances by 2π. Its value is shown in Eq. (4).

$$\lambda_g = \lambda_0/[1 - (f_c/f)^2]^{1/2}, \tag{4}$$

where λ_0 is the wavelength in free space.

The equivalent undulator wavelength, λ_u, is given in Eq. 5 [1, 2].

$$\lambda_u = \lambda_g/(1 + v_p/c), \tag{5}$$

where the equivalent undulator period is λ_u, the wavelength of the oncoming wave is λ_g, and the phase velocity of the oncoming wave is v_p.

As can be seen from Eqn. 3 and 5, the undulator period, can be changed significantly by changing the operating frequency in the vicinity of the cutoff frequency. The equivalent undulator field can be held constant, or, alternatively, the x-ray brightness can be held constant by adjusting the source power.

Figure 4 shows a comparison of on-axis brightness (ph/s/mrad^2/mm^2/0.1%bw) between possible microwave undulators in the HEM_{12} mode and the existing and possible future superconducting wire undulators (SWU) [6]. The storage ring parameters that form the basis for the calculations are those of the Advanced Photon Source storage ring at Argonne National Laboratory.

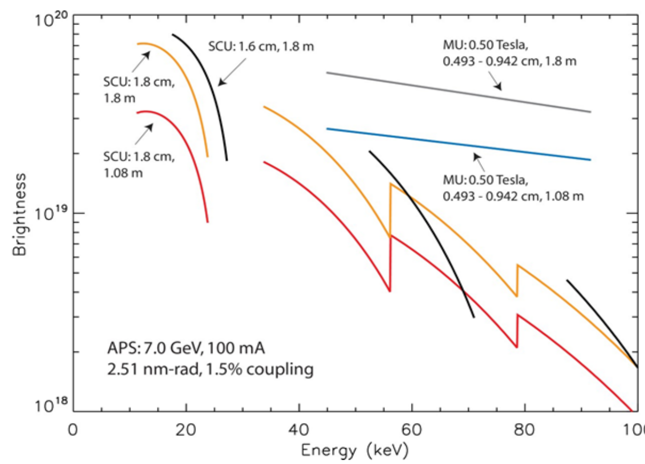

Figure 4: X-ray brightness, ph/s/mrad^2/mm^2/0.1%bw, as a function of x-ray energy for a MU in the HEM_{12} mode over the frequency range of 18-GHz to 24.5 GHz and for 1.08 and 1.8 m long. Comparison plots are also made for the existing APS and possible future SWU (SCU: 1.8cm).

The range in x-ray energy from 45 to 65 keV in Fig. 4 is calculated for an undulator with a = 2.15 cm, b = 2.2 cm, and ε_r = 9.9. The range from 65 keV to 90 keV is calculated for an undulator with a = 1.25 cm, b = 1.3 cm, and ε_r = 9.9.

RF SYSTEM DESIGN CONCEPT

A possible topology for the undulator is a ring resonator (RR) in which the EM wave recirculates back through the MU structure [7, 8]. Power lost by the circulating electromagnetic wave is provided by one, or more, input couplers. Figure 5 is schematic view of the RR structure.

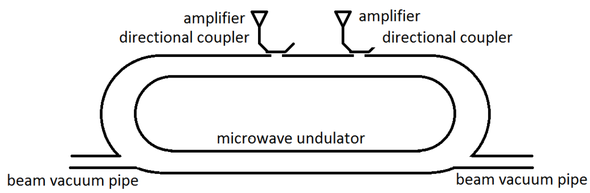

Figure 5: MU in a resonant ring topology.

Since this is a resonant structure, the circulating power is orders of magnitude higher than the input power if the losses are relatively low. Operating the structures around 1.8 to 2 K, the input losses of the MU structure described above in Figs. 3 and 4 range between 125 to 550 Watts per meter to achieve an equivalent undulator field of 0.5 Tesla [5]. The dielectric material must be very low loss at cryogenic temperatures and between 20 to 35 GHz in order to achieve high Q cavities. Sapphire and yttrium aluminum garnet (YAG) are dielectric materials that are suitable since their loss tangents at 4 K are 10^{-7} to 10^{-9} [9,10].

The total power loss will be about 2.5 to 3 times higher when including the return WG of the RR. This level is a factor of ten or more too high for CW operation. With further improvements in developing low loss superconducting surfaces, such as nitrogen treatment of Nb [11] or MgB_2 films [12] to significantly lower the surface resistance, CW operation could become a possibility.

Commercial traveling wave tube amplifiers are available in this frequency range with 2 to 2.5 GHz bandwidths. Their power outputs tend to be a few hundred watts to 1.5 kW, which will require combining two or more amplifiers. To achieve the full tuning range, two sets of TWT amplifiers, configured with waveguide switches, would be needed between the higher and lower frequency ranges of operation. The TWT amplifiers are available in relatively compact rack mounted units and combiners and WG switches are commercially available.

The RR shown in Fig. 5 has two coupling ports. Two, and probably more ports, are required to suppress degenerate modes, i.e. modes with different field patterns and WG wavelengths that are able to propagate at the same frequency. The amplitude and phase at the different input ports are adjusted to maximize the power input to the desired MU mode and to cancel excitation of the degenerate modes. This provides the ability to make the ring excitation wide band to accommodate continuous adjustment of the x-ray energy over the desired range while still suppressing degenerate modes.

The computational technique as applied to an optical RR is presented in a paper by McKinnon et al [8]. Sun applies a similar approach on an optical RR to broaden the bandwidth of a band pass filter [13]. Sun uses passive coupled lines for rejecting side bands. Measured results are provided demonstrating very wide band coupling of the fundamental mode with successful rejection of sidebands. Whereas Sun uses passive coupled lines, active amplifiers with circulators on each port of the MU RR would be used for greater control.

ACKNOWLEDGEMENT

We thank Roger Dejus of the Advanced Photon Source for his calculations of x-ray brightness and the graph showing comparisons of MU options with existing and possible future superconducting wire undulators.

REFERENCES

[1] T. Shintake, K. Huke, J. Tanaka, I. Sato, and I. Kumabe, "Development of microwave undulator," *Japanese J. of Appl. Phys.,* Vol. 22, p. 844-851, 1983.

[2] K. Batchelor, "Microwave undulator," Brookhaven National Laboratory Report, WE3 –12, Upton, NY, USA, 1986, unpublished.

[3] Sami Tantawi *et al.*, "Experimental demonstration of a tunable microwave undulator," *Physical Review Letters 25*, PRL112, 164802, April 2014.

[4] Christopher C. T. Chang, and John W. Dawson, "Propagation of Electromagnetic Waves in a Partially Dielectric Filled Cylindrical Waveguide", *j. Appl. Phys.,* Vol. 41, pp. 4493-4500, 1970

[5] R.L. Kustom, G. Waldschmidt, A. Nassiri, and K. J. Suthar, "Dielectrically Loaded Waveguide as a Short Period Super-conducting Microwave Undulator", *Proc NAPAC2016*, Chicago, IL, USA, Oct. 2016

[6] Brightness calculations and graph, Roger Dejus, Argonne National Laboratory, Argonne, IL, USA, private communication, April. 2017.

[7] Y. Kang, J. Song, and R. Kustom, "A Microwave Beam Waveguide Undulator for a Brilliant Above 100 keV Photon Source", *Proc 1999 Particle Conference,* New York, NY, USA, Mar. 1999. Pp 168-170

[8] W. R. McKinnon, D.-X. Xu, C. Storey, E. Post, A. Densmore, A. Delage,P. Waldron, J. H. Schmid, and S. Janz, "Extracting Coupling and Loss Coefficients From a Ring Resonator", *Inst. For Microstructural Sciences,* Vol. 17, Oct. 12, 2009

[9] V. B. Braginsky, V. S. Ilchenko, "Experimental Observation of Fundamental Microwave Absorption in High Quality Dielectric Crystals", *Physics Letters A,* Vol. 120 pp 300-305, Mar. 7, 1987

[10] Jerzy Krupka and Janina Mazierska, "Single-Crystal Dielectric Resonators for Low-Temperature Electronics Applications", *IEEE Trans. On Micro. Theory and Tech.*" Vol. 48, pp 1270-1274, July 2000

[11] Anna Grassellino, "N doping: progress in development and understanding," *Proc. SRF'2015*, Whistler, BC, Canada, Sept. 2015, paper MOBA06, pp. 48-54.

[12] B. B. Jin, et al., "Microwave and terahertz surface resistance of MgB2 Thin Films," *Journal of Superconductivity and Novel Magnetism,* Vol. 19, pp. 617-623, Nov. 2006.

[13] Sheng Sun, "A Dual-Band Bandpass Filter Using a Single Dual-Mode Ring Resonator", *IEEE Microwave and Wireless Comp. Letters*, Vol. 21, June 2011, pp 298-300